Optimum Illuminant Determination Based on Reduced and Optimized Multispectral Spectroscopy to Enhance Vein Detection

By

Pavanjeet Singh Sidhu

14909

Supervisor: Dr. Walter Nicholas

Co-Supervisor: Dr. Naufal M. Saad

Final Dissertation

Final Year Project II – Term Jan. 2015

Centre of Intelligent Signal & Imaging Research (CISIR) Cluster

Department of Electrical & Electronics Engineering

University of Technology PETRONAS

Malaysia.

Abstract:

Venepuncture as a mode of gaining intravenous access has been a prime practice in surgical procedures and other conventional drug administering into a patient. Biomedical engineering has stressed relatively high scale of importance in the spectroscopic analysis of vein imaging as a sparky approach to promote a non-invasive catheterization. However, medical personnel are challenged by the physiological circumstances of skin tone, presence of scars and irregularity of the epidermal topology, when performing subcutaneous vein localization, which led them to increase number of insertion attempts. Hence, this paper proposes an optimized solution to provide enhanced visual aids for personnel to achieve successful vein catheterization at first attempt. Vein localization using various stages of formulated analysis; multidimensional array pixel evaluations using intensity and reflectance contrasts using CLAHE algorithm are performed in the Near Infrared spectral band as a novel study to produce an automated illuminant selection for an enhanced vein visualization. Subjects of study are categorized in four separate classes based on their Luminance value of each skin tone to extract the optimum illuminant parameter for each category on a reduced spectrum. The intensity and reflectance contrast datasets obtained deduce the selection of the best illuminant value at which the contrast anticipated will be the highest. Results from modelling will be translated in to a prototype system called the Smart Vein Locator, which will autonomously select the best illuminant based on different topological factors of the subject.

KEYWORDS: Near Infrared, Spectroscopy, Intravenous (IV) Catheterization, optimum illuminant, wavelengths, Contrast-Limited Adaptive Histogram Equalization (CLAHE), Reflectance.

Contents

List of Tables

List of Figures

Nomenclature

NIR	Near Infrared
DAQ	Data Acquisition Card
IV	Intravenous
ROI	Region of Interest
SNR	Signal-to-Noise Ratio
VCE	Vein Contrast Enhancer
IR	Infrared
MATLAB	Matrix Laboratory
BVP	Backward Variance Propagation
CLAHE	Contrast-Limited Adaptive Histogram Equalization

1.0   INTRODUCTION

1.1   Background

Studies till date have underlined venepuncture or catheter insertion into a patient as an essential yet a crucial practice in the biomedical fields; where administering drugs and acquiring blood samples are crucial point-of-care applications [1], for pathological analysis requires the intravenous (IV) catheterization. At this present day, these practices are still performed manually by medical personnel and it is envisioned to be superseded by an automated technology.

The cardinal drive for the evolvements in this narrowed area of study in phlebotomy imaging is to ensure a non-invasive blood vessel localization and catheter insertion; so as to counter pain and extravasations imposed onto the patient's integument.

The Near Infrared (NIR) light's spectrum serves an effective propagation characteristic in retrieving spatial variable data in tissues and blood volume present in the region of interest (ROI) of a skin, based on their spectroscopic optical absorption coefficient. Due to low absorption characteristics of the hypodermal environment (i.e. oxy- (HbO_2) and deoxyhemoglobin (HbR), melanin and H_2O) in the Near Infrared spectrum, penetration of light rays in the hypodermis layer are at its peak [2], enabling subcutaneous vessels localization.

Multispectral approaches has been used to enhance vein images, but provided no liable estimation of varying physiological properties of skin surfaces, like skin tone and topological factors like marks and hair presence. Subjects of dark skin tone complicates the classification of illuminants, resulting in poor and ambiguous results of vein contrasts.

This extended documentation presents the progress of the initiative of utilising the multiple high-speed IR emitting diodes prototype to compliment with the simulated multispectral image results, to select the optimum combination of wavelengths, λ (illuminants) classifications of varying skin tones of different subjects, to deduce the precise vein contrast. This concept is proven by a holistic identification study on the trait given discretely by each wavelength in the electromagnetic spectrum towards the clarity of venous enhancement, taking into consideration the reflective nature of the physiological environment on the outermost layer of the integument.

1.2 Problem Statement

Barton, et al. [3] studied that 2.18 catheter insertions are required on an average patient without assistance from vein localizing technologies. Infants are the majority of patients who suffer from the multiple unsuccessful catheterization attempts, which lead to tissue infiltration and extravasations, triggering potential surgeries due to diffusion or accumulation of administered substance in the tissue [4]. This paper addresses the biomedical complexity with a real-time visualization approach to aid in vein detection. This study analyses 40 subjects or patients classified into FOUR (4) categories of skin tones with respect to their Luminance (L) values [26], retrieving the best illuminant for each category. This study is done within the multispectral band range window of 412nm to 1027nm, (with a spectral resolution of 2nm) which is the specification of a multispectral image taken from a Specim® spectral camera. This reduced spectroscopic modelling of THREE stages enable an automated selection of illuminant during a real-time experimentation, by translating the illuminant into High Speed Infrared LED to be installed in the existing Smart Vein Locator prototype. The sequential modelling process takes on a tedious procedure to extract the highest reflectance contrast information contributed individually by both vessel and skin tissue information on a randomly selected ROI, across 700nm-950nm spectrum. The final stage deduces the functionality of the Contrast-Limited Adaptive Histogram Equalization as an efficient enhancement scheme to aid in automatic vessel extraction with its contrast limiting algorithm.

1.3   Objectives & Scope of Study

This study is to develop an automated classification of patient's skin surface traits in function of the luminance reflected from their skin colour based on a reduced spectrum, eliminating ambiguities in classifying physiological factors present in venous imaging and enhancing the contrast in resulting images. This research analyses the multispectral image of a subject's forearm retrieved from the Specim® multispectral camera, in order to evaluate the information of the vessel pixel to the function of skin tissue and background reflectance. This analysis is to further improve the precision of NIR wavelength range of selection, in discriminating the venous and skin topological illuminants. This study uses EIGHT subjects of each skin tone in all FOUR stages of spectroscopic modelling to attain a high percentage of accuracy for computing, analysing and constricting the precision of wavelength selection(s) on a reduced spectroscopy. The best illuminant (wavelength) selection is capable of enhancing the visibility of the venous contrast, respect to the physiological disturbances and reflectance noises along the NIR spectrum of study. This study will further contribute to illuminant unification (best selected single wavelength) as an illumination device will be mounted on the Smart Vein Locator prototype, once the developed concept of modelling is proven with favourable trends from all THREE stages of modelling.

DESIGN	A dummy circuit of High-Speed Infrared LED's is built as an experimental modelling approach correlating to Stage II Empirical Modelling to physically deduce the best illuminant for the particular ROI, where the vessel segment is best discriminated from the skin tissues, in a real time imaging.
MANIPULATIVE FACTOR	Thirty-two subjects of multispectral images were modelled to hypothize the optimum illuminant selection for best clarity of vessel contrast respect to skin tissue and background ROI reflectance index. ROI of study were subjected to various topological parameters, such as, scars, skin color, pigmentations, tattoos and presence of hair, which contributed a fairly high disturbance to the multidimensional modelling.
EXPECTED OUTCOME	Automated classification of illuminant as a contrast enhancer in real-time vein detection imaging, using the Contrast-Limited Adaptive Histogram Equalization (CLAHE) algorithm, which extract the peak reflectance contrast of all subjects from all classes of skin tones (Fair, Light Brown, Dark Brown and Dark).

Figure 1: Illustrative description of the scope of study of this research

2.0   LITERATURE REVIEW & THEORY

In the early stages of blood vessel spectroscopies, vein detection in dark pigmented skins served high difficulties to the naked eye [5] and introduced inaccurate vein depth and diameter information at the enhanced vein contrast projections [6].

The theory of wave propagation in biological tissues is infused into biomedical imaging to localize subcutaneous veins sitting in the hypodermal layer of the integumentary structure. One of the branches of this theory is the optical tomography which offers a non-invasive, cost effectively repeatable and experimentally simplified method of vein contrast imaging and enhancements [7].

2.1 NIR Imaging in Vein Localization

NIR imaging is a derivative of a light propagation property where it possesses the behaviour of reflectance, absorptivity and sparse (scattering) which sits at the range of 650nm-940nm (0.78 to 2.50 microns) [8] of the electromagnetic spectrum. Looking at the quantum mechanics [9], overtone and combination vibrations of the CH-, OH-, and the NH- molecules are constrained to a specific band window of vibration energy. Compared to other electromagnetic mediums, NIR display a versatile property of electronic and vibrational transitions. NIR is unique from its neighbouring spectrums due to its weak overtone and combination modes which are forbidden transitions at this range. Hence, this trait gives the NIR band a fairly large
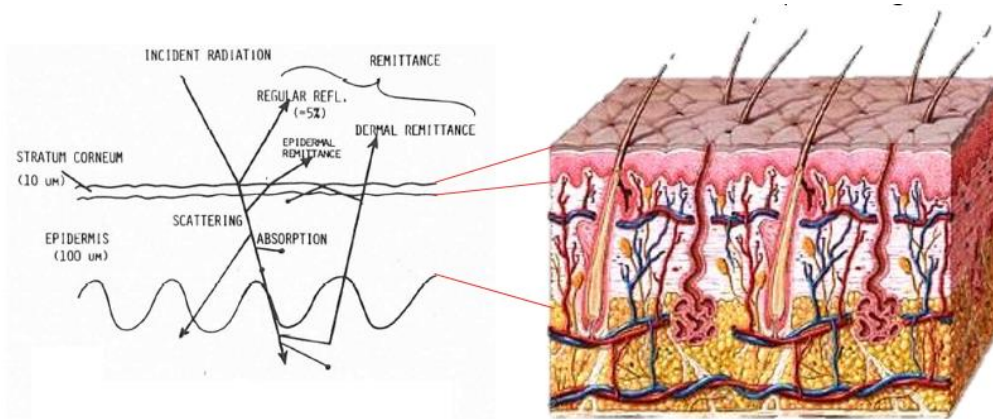
Figure 2: NIR behaviour in human skin optics [10]

transition window to rays of high frequency (radiation). This deduces an undisrupted travel of light within the NIR regions, where absorption will be low.

The principle of NIR application introduced in this study is based on the **Beer-Lambert Law**, which defines the correlation of chemical's strength of light **molar absorptivity, ε** with the given **pathlength, l** following the formula (1):

$$A = \varepsilon c l \qquad (1)$$

Where A is the **actual absorbance**. NIR's versatility in the integumentary system, as illustrated in Figure 2, explains its ability to penetrate deep into the hypodermal layer of the system, where chromophores H_2O (Water), HbR (De-Oxygenated Hemoglobin) and HbO_2 (Oxygenated Hemoglobin) have a relatively low absorption strength in that transition window. This characteristics enables extraction of vascular information, which contributes to computed-

tomographic (CT) studies, resonance imaging and the most anticipated, subcutaneous vessel localization.
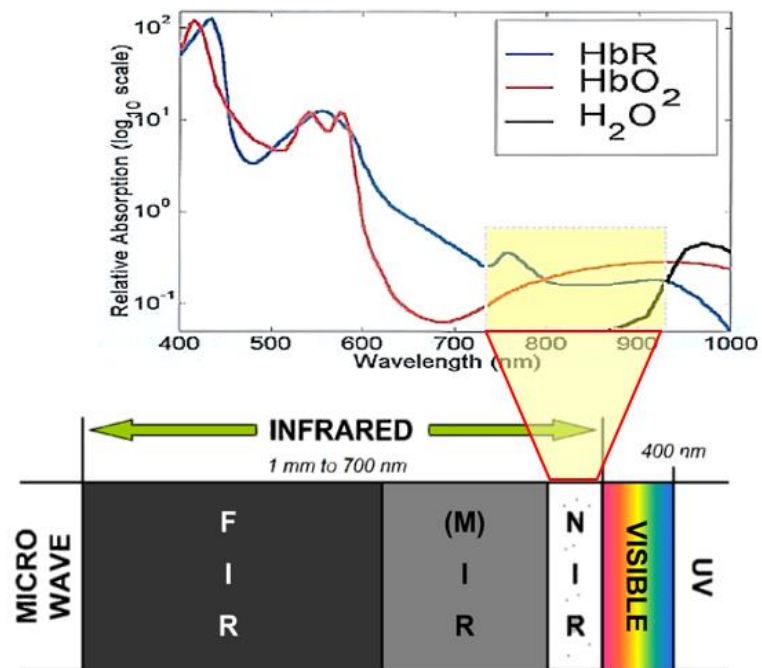
Figure 3: Relative absorption characteristics of chromophores in the NIR band. [2]

2.2   Comparative Analysis of Previous Literature

The literature of Shahzad, et al. [11] studies, phlebotomy localization is done using three theories, namely, Transillumination [12], Combined Photoacoustic and Ultrasonic [13] and Near Infrared Imaging Technique. Transillumination procedure returned a drawback since it required the need of direct contact of device on the patient's skin which may risk spreading of viruses or diseases from one patient to another. The use of single selection of wavelength in this method offered unfavourable results in veins localization. The Photoacoustic method provided vein depth and diameter parameters but failed to identify its positioning and shape, due to its tendency of generating noise, as a consequence of reduction in the signal to noise ratio (SNR) [14].

The Near Infrared imaging method, whereas, works on the theory of light propagation, which possess absorption, reflection, refraction and sparse behaviour has a high penetration ability in the low absorption coefficient range of the hypodermis layer [2, 11, 15].
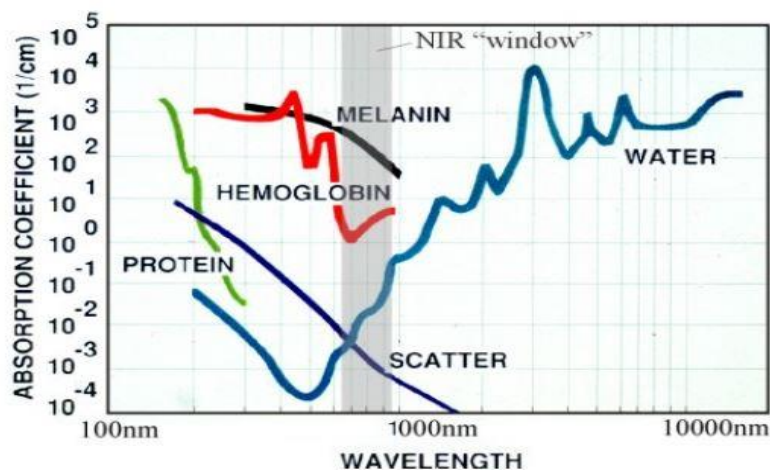
Figure 4: Molar Absorptivity behaviour of chromophores in NIR.

The curve above *(Figure 4)* shows the relatively low absorption coefficients of primary light absorbers called chromophores (oxyhemoglobin, HbO_2, deoxyhemoglobin, HbR and water, H_2O) in the NIR window [11, 16]. In the perspective of the absorption and reflectance characteristics of the skin and the chromosphores (in this case the deoxyhemoglobin, HbR of the subcutaneous veins), both skin tissues and HbR can be distinguished significantly from their respective resultant images, where veins appear darker compared to the skin tissues due to the former's high absorption coefficient at the NIR window [17].

Zeman, et al. [18] pioneered the Vein Contrast Enhancer (VCE) and the VeinViewer which captures the multispectral image of skin in the Near Infrared (NIR) spectral range, projecting back greater than 0.06mm enhanced vein image [19] onto the skin surface as an aid for venepuncture.

However, Paquit, et al. [20] criticised this prototype as it suffered minimal functionality in estimating the relative depth or diameters of veins present on the enhanced image projection, and decreased in performance based on ambiguity in classifications of varying skin tones. Early researches in multispectral vein imaging have evaluated the best NIR wavelengths selection for the optimum vein contrast in subject to the manipulated variables such as skin colour, presence of hair on the forearm surface and varying skin topography. However, Wang, et al. [21] hypothecated the use of single-wavelength methods in the preliminary researches had many limitations addressed in the multispectral vein detection due to the back ground skin reflectance and post-processing algorithms [20-22]. Its single wavelength of 740nm resulted in an evidently poor variation light wave penetrations into the skin tissues [15].
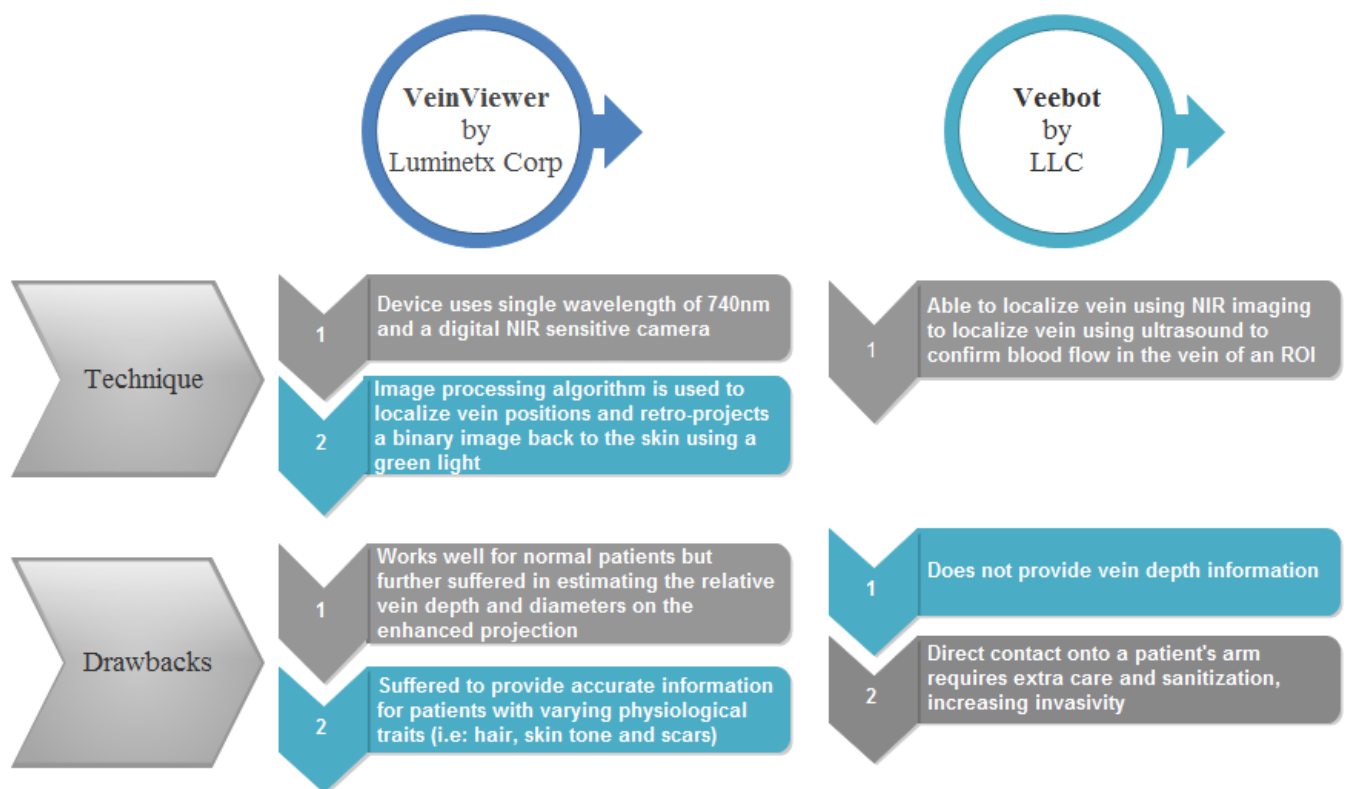
Figure 5: Comparative deduction of techniques and shortcomings of previous NIR studies [18-20]

To counter these complexities of physiological factors in phlebotomy imaging subject to skin curvatures, vein depth and diameters, Nishidate, et al. [23] came up with the Monte Carlo modelling theory, using diffuse reflectance images of the region of interest (ROI) to locate and measure depth and diameters of veins at multiple wavelength parameters. The following problem statement here remains to be the accurate classification of the varying subject skin colours into four categories of dark, dark brown, light brown and fair. Shahzad, et al. [11], [15] uses the principal component analysis (PCA) to compute the Eigen vectors of retrieved high-dimensional multispectral images analysed on a reduced spectrum, to define the optimum wavelength combination within the NIR range used to illuminate the ROI.

2.3 Comparative Analysis of Previous Researches in Vein Imaging using Different Techniques

Theories	Transilluminance	Combines Photoacoustic & Ultrasound Technique
Technique	Uses single wavelength from the visible range of the electromagnetic spectrum	Light and ultrasound waves to obtain real-time high resolution image of veins
Available Prototypes	*Veinlite*, *Venoscope*, *Wee Sight* and *Vein Locator*	
Technique Shortcomings	- Need of **direct contact** with the skin of the patient which may lead to spread of viruses from one patient to the next. - Costly cleaning and disinfection processes before using on the next patient **Single visible wavelength illumination** used in this devices are not of high precision in terms of localizing veins in all the cases due to **low penetration capabilities** in the hypodermis.	- Provide depth and diameter information of the vein, **BUT** not about the position, shape and orientation - This technique has a high **tendency of generating an echo signal** (*spread noisy waves*), which reduces the returning signal's SNR **High expenses** due to usage of ultrasonic gel which aids in ambient noise reduction

.

Table 1: Comparative implementation of different techniques [24]

3.0 METHODOLOGY

This documentation presents a sequential progress of modelling and analyses to develop a theory of optimum illuminant identification as a projection aide for real-time vein imaging, as an initiative to serve the biomedical field in the initiative of encouraging medical practices to be done non-invasively.

This analysis is performed by modelling the contrast of multispectral images using MATLAB, which normalizes the three-dimensional subject image data into two-dimensional mean image. The Stage I of analysis will be the computerization of contrasts from the Reflectance (R) properties of the subjects. This modelling proves the property of light reflectivity at the arbitrarily-modelled Near Infrared wavelength respect to the absorptivity coefficient of vein and melanin (skin), which deduces which NIR spectrum/range/value contributes to the optimum vein enhancement of any experimented multispectral image regardless of its Luminance (skin tone or topology) characteristics.

The reflectance images computed is then Gaussian-smoothed with 26 wavelength Gaussians of 700nm to 950nm to empirically deduce vessel contrast clarity of all Gaussian-smoothed images. This stage of modelling is the Stage II – Empirical Modelling, where the results of the modelling are 2D smoothed images, which physically display at which wavelength the vessel contrasts seem to be at its best clarity and which wavelength value contributes to noises.

Stage III is the final modelling stage, where this stage is a tremendous improvisation of the previous modelling process, with an added formulation known as Contrast-Limited Adaptive Histogram Equalization (CLAHE). The CLAHE algorithm enhances contrast of every pixel scatter on an image ROI, which in turn, improves the vessel discretization respect to the skin tissues. Hence, Stage I Reflectance Modelling is repeated on the CLAHE formulated images to observe the best selection of illuminants, based on the study on 32 different images of different skin tones and topological behaviours.

The comprehensive elaboration of the sequential methodology will be further explained in the Results & Discussion section of this documentation.
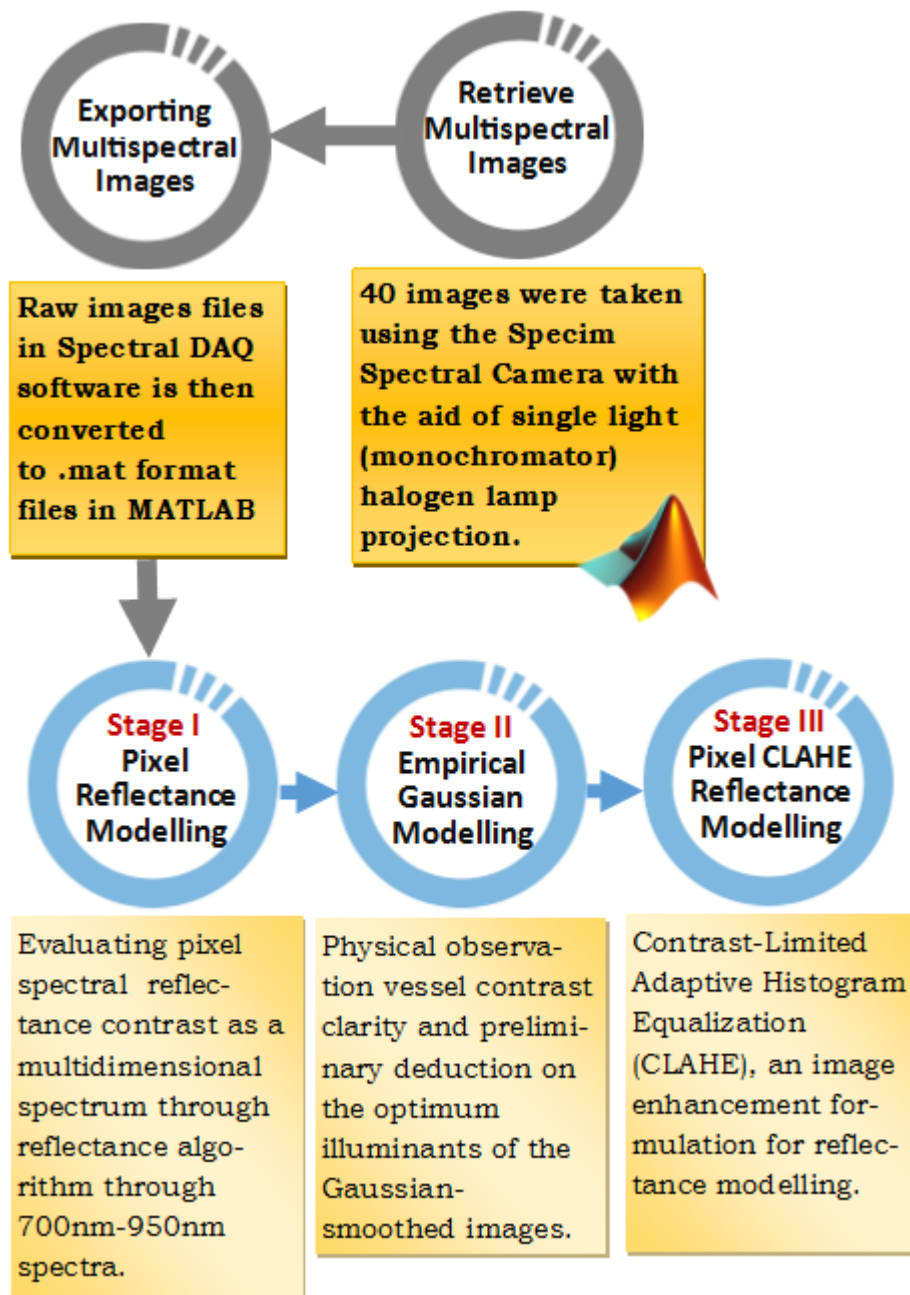
Figure 6: Methodology of vein localization technique

.

3.1 Data Acquisition

Since this study requires acquisition of vessel information in a NIR spectroscopy, subjects were acquired (captured) using a Specim® multispectral camera, which functions under a specifications of spectrum range between 400nm to 1000nm, with a 2nm resolution. Utilisation

of halogen lamps widened the spectrum of study from 350nm to 2500nm, providing suitable lighting condition for capturing lower arm area of the subjects.

Figure 7: Specim® multispectral camera
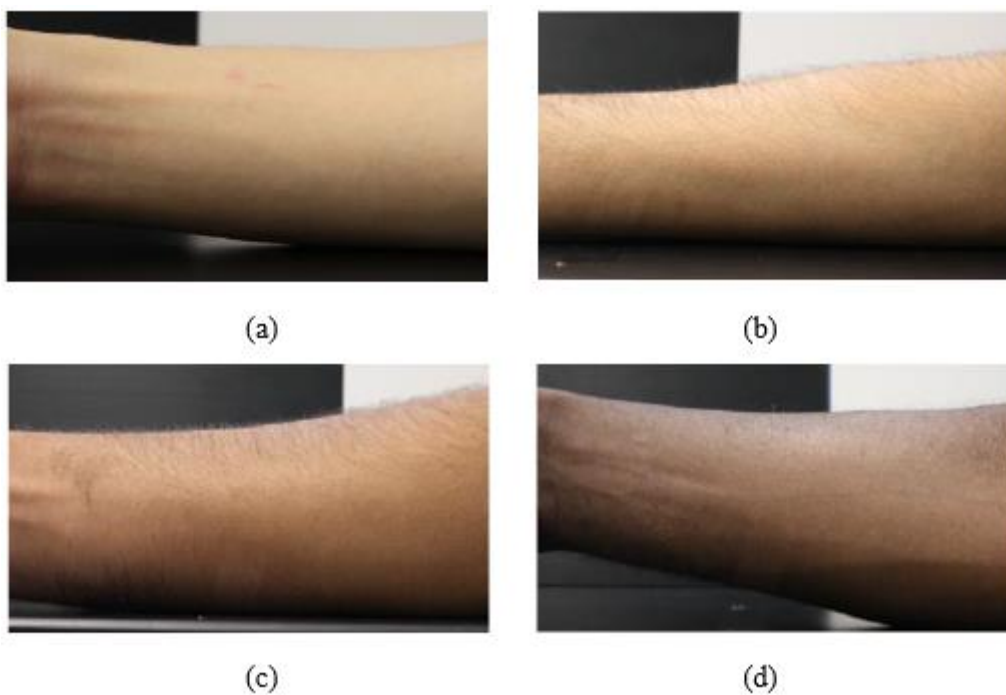
Figure 8: Four categories of skin tone based on the Luminance band. (a) Fair category, (b) Light Brown Category, (c) Dark Brown Category, and (d) Dark

Subjects were classified into four categories based on the intensity of the Luminance they projected onto the Chroma Meter which registers the *L*, *a*, and *b* parameters of the subject's skin [26]. The classification of subjects are displayed in Figure 8. However, spectral images

were translated into .mat files which loads as grayscale multi-dimensional images, ready to be studied on.

3.2   Tools & Software Required

- MATLAB to process multispectral images through algorithms, to parametrize image behaviours and autonomously classify them.
- Specim® multispectral camera to retrieve still multispectral images for modelling purpose – available in CISIR Centre, Block 22.
- Smart Vein Locator, a ready head-mounted glasses, in which, the illuminant source on it is to be improvised through this research - available in CISIR Centre, Block 22.

3.3   Flow Chart
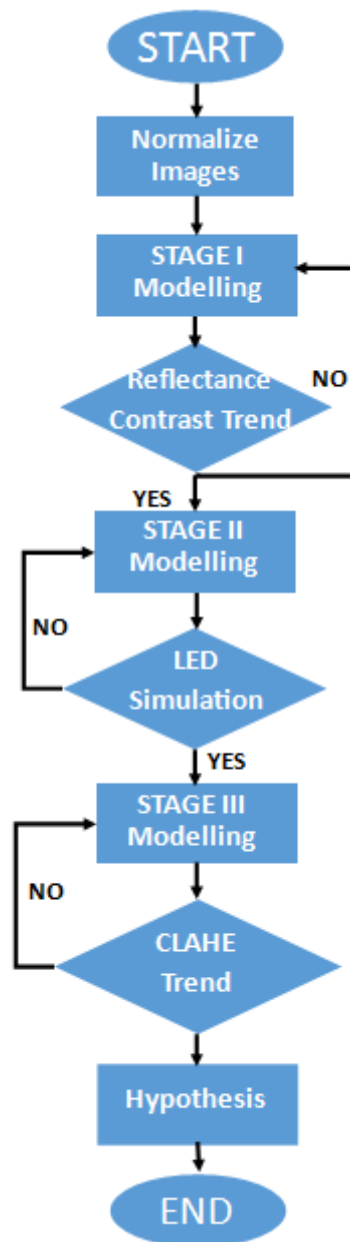
Figure 9: Flowchart of anticipated outcome from research

3.4   Project Gantt chart & Planned Future Expansion

Activity	Week 1	2	3	4	5	6	7	8	9	10	11	12	13	14
Selection of FYP Title	■	■												
Prelimenary Research and Scope Determination		■	■	■										
Literature Review				■	■	■	■	■	■	■	■	■	■	■
Extended Proposal						▇								
Vein Reflectance-Contrast Modelling							■	■	■					
Proposal Defense Presentation									▇					
Logging Data of Contrast for all subjects										■	■	■		
Incorporation of Reflectance algorithm												■	■	
Submission of FYP 1 Draft Interim Report													▇	
Submission of FYP 1 Final Interim Report														▇

■ **Key Milestone** (red)

■ **Gantt Chart Activties** (yellow)

Table 2: Final Year Project Term I Gantt chart

Activity	Week 1	2	3	4	5	6	7	8	9	10	11	12	13	14
Incorporation of Frangi Vesselness Filter algorithm	■	■												
Integrate Reflectance into te Frangi Filter			■	■	■	■								
Reflectance data acquisition and classification						■	■	■						
Progress Report Submission								▇						
Deciding/Selecting Best Illuminant (Wavelength)									■	■				
Testing on real-time subjects										■	■			
Result Analysis											■			
Pre-SEDEX Presentation											▇			
Future Work Recommendation											■			
Draft Report Submission												▇		
Final Report Submission													▇	
Viva														▇

■ **Key Milestone** (red)

■ **Gantt Chart Activties** (yellow)

Table 3: Final Year Project Term II Gantt chart

4.0 RESULTS & DISCUSSIONS

The proof of concept of utilising more than one wavelength as the illuminant source is deduced to have produced an accurate classification of best contrasts for each category of skin tone, based on Luminance [26] bands. Luminance is the luminous intensity at the particular ROI, where brighter skin complexion will register a higher index of *L*. The concept Luminance derives from the Leibniz's notation which defines it as follows:

$$L_V = \frac{d^2 \emptyset_V}{dA \, d\Omega \cos \theta}$$

Where:

L_V is the luminance in unit cd/m^2.

$\emptyset_V$ is the luminous flux.

θ is the angle between normal line and fixed direction of light motion.

A is the area of the ROI in unit m^2.

Ω is the solid angle.

4.1 Modelling Stage I – Spectral Reflectance Algorithm

The spectral reflectance algorithm is incorporated into the image modelling to extract the spectral reflectance index of each image and subsequently modelled across a range of illuminants within the band of 700nm-950nm to observe if this algorithm extracts the characteristics of each skin tone uniquely, through the vessel against skin tissue reflectance contrast trend computed at the end of this modelling.

Reflectance is expressed as:

$$R(x, y, \lambda) = \frac{E_{reflected\ (x,y,\lambda)}}{E_{received\ (x,y,\lambda)}} \tag{2}$$

R(x, y, λ) denotes reflectance index along *(x, y)* coordinates of an image across a set of λ, where it represents the ratio of reflected energy to received energy of a medium.

The raw intensity parameters *I(x, y, λ)* by the multispectral experimental conditionings at point *(x, y)* across a set of λ can be represented as the following equation:

$$I(x, y, \lambda) = L(x, y, \lambda)S(x, y, \lambda) \times R(x, y, \lambda) + O(x, y, \lambda) \tag{3}$$

L(x, y, λ) is the luminance vector, *S(x, y, λ)* is the spectral response of the multispectral camera setup and the *O(x, y, λ)* offset which contains the dark current and stray lighting setup of the experiment.

The experimental imaging setup conditioning of Lambertian white and black background surface develops white and black reflectance constants of $R_w(x, y, \lambda)$ and $R_b(x, y, \lambda)$ registering 0.98 and 0.05 respectively. Hence, substituting these two constants will eventually compute the $I_W(x, y, \lambda)$ and $I_{B}(x, y, \lambda)$ constants.

Then, *L(x, y, λ)* × *S(x, y, λ)* can be obtained against a set of wavelengths discretely.

$$L(x, y, \lambda) \times S(x, y, \lambda) = \frac{I_W(x, y, \lambda) - I_B(x, y, \lambda)}{R_W(x, y, \lambda) - R_B(x, y, \lambda)} \tag{4}$$

By substituting equation (4) into equation (3), the offset parameters will be produced:

$$O(x, y, \lambda) = \frac{I_B(x, y, \lambda) \times R_W(x, y, \lambda) - I_W(x, y, \lambda) \times R_W(x, y, \lambda)}{R_W(x, y, \lambda) - R_B(x, y, \lambda)} \tag{5}$$

L(x, y, λ) × *S(x, y, λ)* and *O(x, y, λ)* constants are substituted in equation (3) to obtain resultant reflectance for each subject modelled.

$$
\begin{aligned}
R(x, y, \lambda) \\
= \frac{\{I(x, y, \lambda) - I_W(x, y, \lambda)\} \times R_W(x, y, \lambda) - \{I(x, y, \lambda) - I_W(x, y, \lambda)\} \times R_B(x, y, \lambda)}{I_W(x, y, \lambda) - I_B(x, y, \lambda)}
\end{aligned} \tag{6}
$$
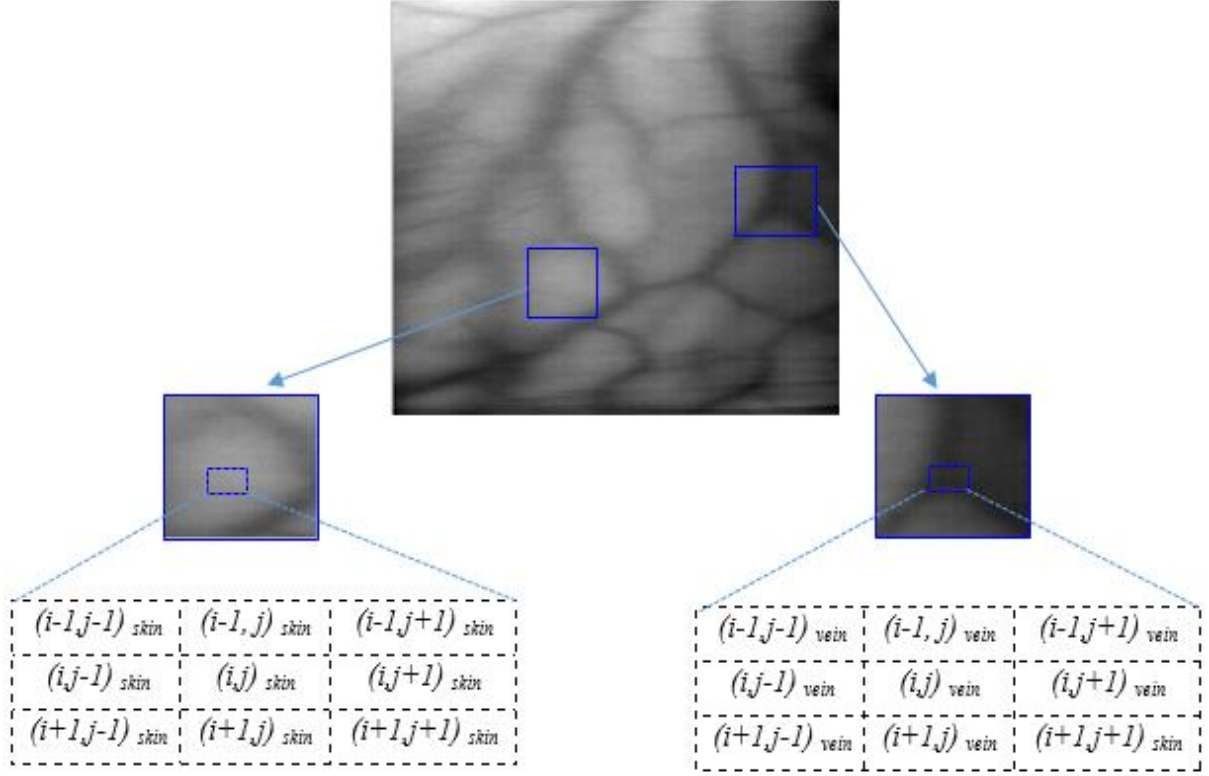
Figure 10: Pixel characterization matrices between vein and skin ROI

This figure displays pixel quantification in terms of reflectance weightage distribution across the ROI's pixel matrices. For each patient, the central and neighbouring pixels within a selected skin or vein region are averaged to obtain the reflectance index of respective homogenous information. Discriminating the skin and vein ROIs by computing the mean value of reflectance will extract the contrast information of the vessel with respect to its background topology, in this case the skin tissue. N values of ROI's of both vein and skin tissue were extracted and meaned to identify the accurate reflectance index of each patient image. Therefore, evaluating an accurate contrast for the simulated LED images. In this scenario, mean intensity of the vein ROI is computed as.

Equation 7 and 8 show the computation for skin and tissue ROIs reflectance index values for N patient in a specific group, respectively.

$$\sum_{x=1}^{N} R_{Skin} = R_{SkinROI}(i,j)_{x=1} + R_{SkinROI}(i,j)_{x=2} + \cdots + R_{SkinROI}(i,j)_{x=N} \quad (7)$$

$$\sum_{x=1}^{N} R_{Vein} = R_{VeinROI}(i,j)_{x=1} + R_{VeinROI}(i,j)_{x=2} + \cdots + R_{VeinROI}(i,j)_{x=N} \quad (8)$$

The final contrast between skin and veins computation for a specific skin tone can be formulated as follows:

$$C_R = \frac{1}{N}\sum_{x=1}^{N} R_{Skin} - \frac{1}{N}\sum_{x=1}^{N} R_{Vein} \qquad (9)$$

Subsequently, the contrast parameter is produced from each slice of image across the Gaussian function of wavelengths, where a trend characterization is made.
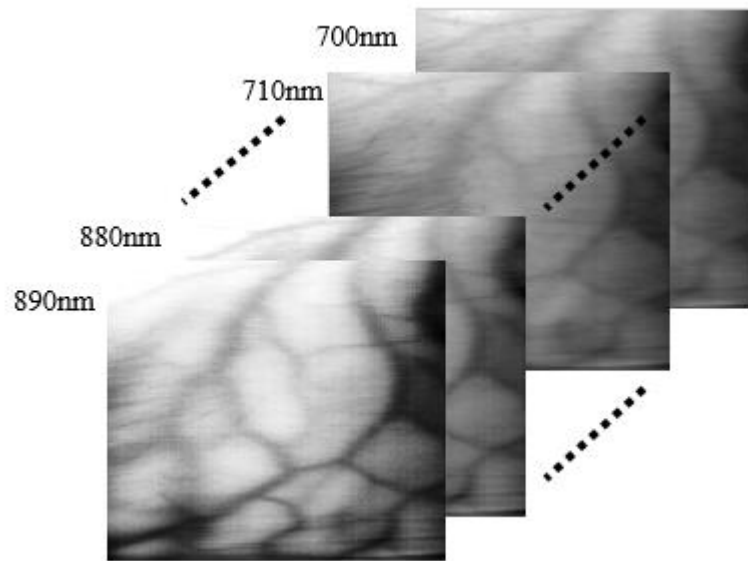
Figure 11: Multispectral image slices in 10nm of spectral bandwidth
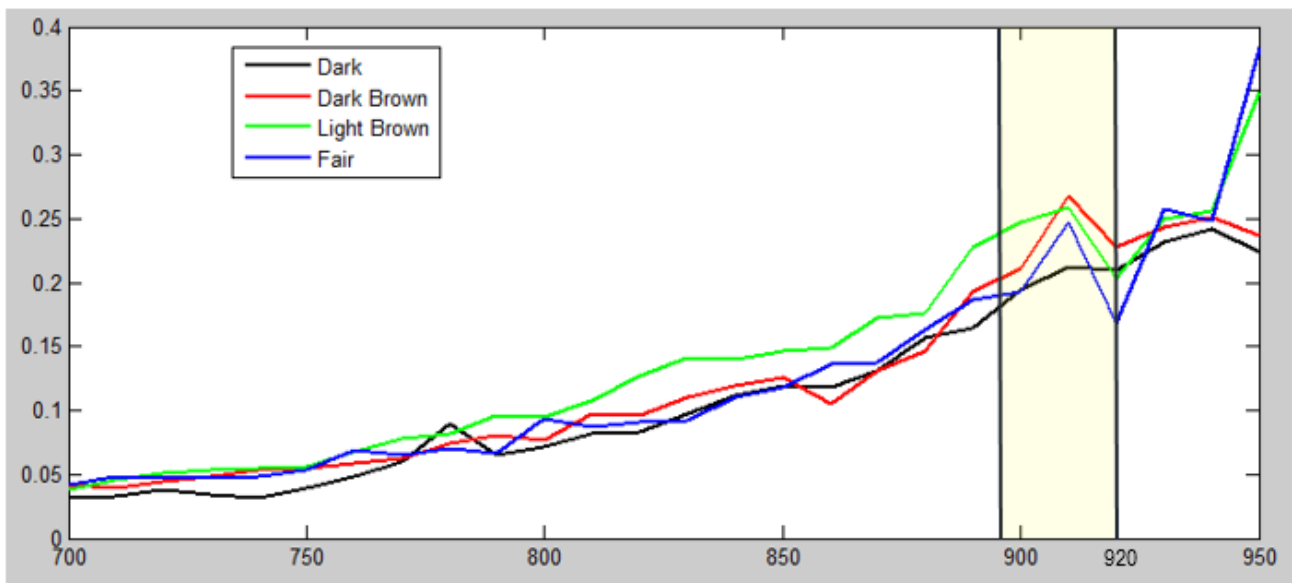
Figure 12: Trend for Reflectance Contrast of 8 Multispectral Images of each skin class; Fair, Light Brown, Dark Brown and Dark

19

Figure 27 indicates best contrasts of vessels at the window of approximately 890nm till 920nm, where beyond that window, the trend experiences extremely high overshoots due to relatively noises present on the image at those slices of wavelengths. The trend experiences gradual increase in contrasts from 700nm till 890nm where the clarity of the vessel contrast enhancement increases as well.

The presence of noises and unnecessary spikes beyond 920nm are due to the absence of histogram equalizations over the image pixel scatters, where a large region of homogenous property (i.e. skin tissue pixels) possess a large intensity index and in turn a large value of reflectance. Hence, image tend to over-amplify noises in highly homogenous areas. Typically, average reflectance index of skin is 220 and 30 for vein. Above 920nm, the image pixel equalization deteriorates, where single pixel index to the neighbouring pixels of a selected ROI, experiences a large deviation in reflectance index (at least 4-5 times). A tile of high reflectance homogenous skin information is prone to strong noise spikes, which results in large variability in the contrast trend above 920nm, as displayed in Figure 27.

4.2   Modelling Stage II - Gaussian-Smoothing Algorithm

The Gaussian Smoothing operation functions in a two-dimensional convolution computation where, two arrays of pixels of identical dimensions, but different intensities are multiplied together to produce a new array of numbers of identical dimension.

This algorithm is to utilise the 2-D resultant normalized multispectral image as a point spread function (PSF) which is developed through a convolution operation.
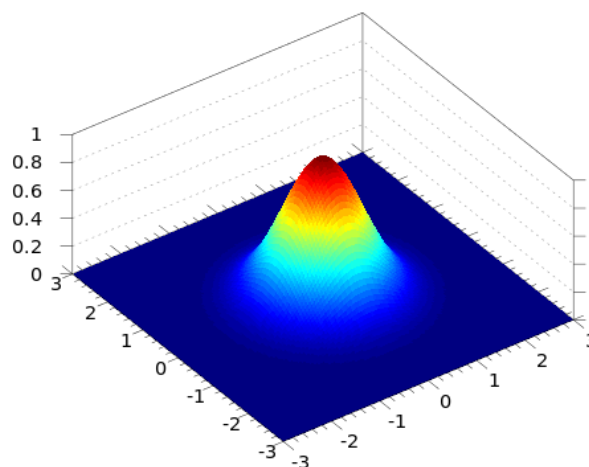
Figure 13: 2-Dimensional Gaussian distribution with μ=0 and σ=1

The empirical modelling using Gaussian-smoothing with FOUR values of illuminants (830nm, 850nm, 890nm and 940nm) were an early identification of multispectral image reflectance trending, where contrast of the entire image was computed. This stage of modelling is to verify the effect of High Power Infrared Emitting Diode as a localization aid for vessel contrast extraction during real time imaging using the Smart Vein Locator.
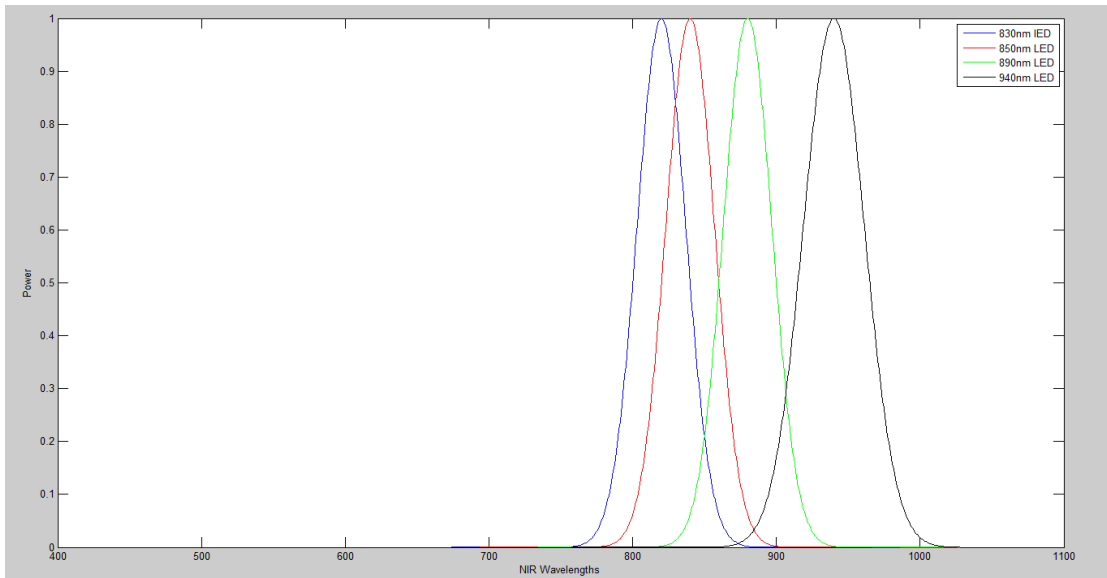
Figure 14: Gaussian functions of 830nm, 850nm, 890nm and 940nm illuminants

Hence, in retrospect of the previous study, a new phase of modelling is produced which quantifies the discriminate of the vein and skin pixel region individually, to observe the trend of contrast across the range of the NIR spectrum window. This stage of study examines the visualization analysis of a multispectral image across wavelength slices of 750nm till 950nm. For this modelling, number of sets of Gaussian NIR wavelengths were increased to increase precision of visualization hypothesis. This stage indicates a rough visualization of image's behaviour under 26 sequential wavelengths, and how the NIR spectrum segregates vessel-skin information.
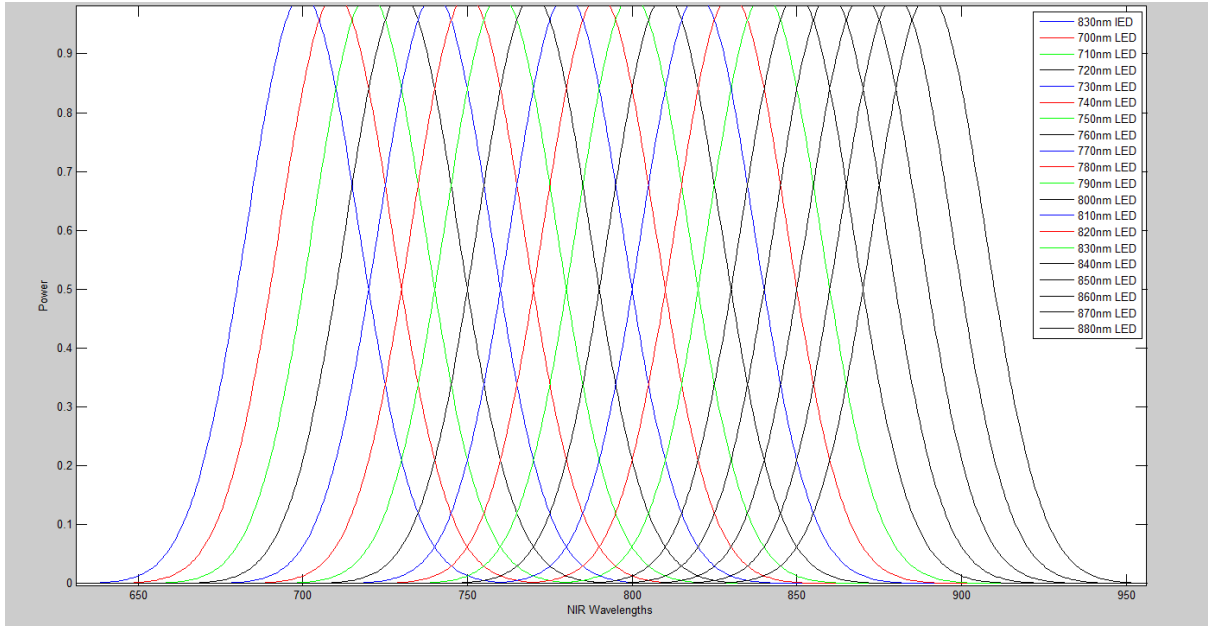
Figure 15: Gaussian function curves of illuminants range of 700nm-890nm with a step increment of 10nm

The Gaussian function which has been incorporated in this study is as follows:

$$f(x) = a\ exp\left(-\frac{(x-b)^2}{2c^2}\right)$$

The *c* parameter is Full Width at Half Maximum (FWHM) where its relationship is showed as follows:

$$\text{FWHM} = 2\sqrt{2\ln 2}\ c \cong 2.35482c$$

The parameter *c* can also be defined as the dual inflection points on the function, which too acts as a bandwidth at *x = b - c* and *x = b + c*. This analytic function gives a zero when x approaches infinity.

Provided the Gaussian is the probability density function of a normal distribution, where the *b* parameter will be mean, μ and the *c* parameter will become variance, σ, then the function becomes a probability Gaussian function of:

$$g(x) = \frac{1}{\sigma\sqrt{2\pi}}e^{-\frac{1}{2}(\frac{x-\mu}{\sigma})^2}$$

The parameter *x* denotes the set range of the wavelengths in the NIR window, μ will represent the wavelength selection of the filter and the σ represents the standard deviation of NIR

22

bandwidths which differ from one spectrum to another. For the High Power Infrared Emitting Diodes with wavelengths from 700nm till 890nm registers an σ of 16.982349 whereas, from 900nm and beyond registers 21.2330451. This specification is stated the datasheet from Vishay Semiconductors manufacturers.
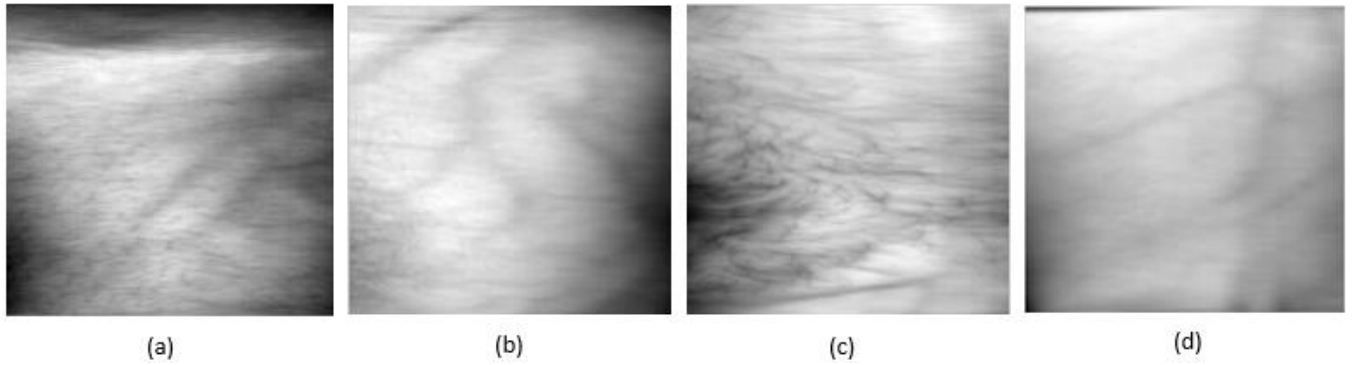
Figure 16: Raw multispectral image of subject with (a) Dark skin tone (b) Dark Brown skin tone (c) Light Brown skin tone (d) Fair skin tone

The Gaussian function of these four illuminants, 830nm, 850nm, 890nm and 940nm were Gaussian-smoothed with all forty subjects to develop a dataset of contrasts which deduces the behaviour of the vein contrast respect to different illuminant, λ sources. This stage is a stage of preliminary physical observation of the behaviour of vein localization in the NIR spectrum. Hence, these four illuminant values were pre-selected as there were only these available High-Speed Infrared LED's of Vishay Model, which were translated into a dummy circuit shown in the last section of this dissertation.

The results of this analysis are displayed in the following. The results to be displayed in this documentation shows the behaviour of a selected subject from each category of skin tone, and the improvements on the ROI's vein contrast, as compared to the pre-enhanced images as shown in Figure 10. The modelling phases are divided into THREE phases. It is observable that the vessel information is fairly enhanced to a visible state. However, human visualization is never a benchmarking factor in determining image quality, hence, sequels of modelling stages were implemented to further enhance the extraction of vessel information with respect to the skin tissue which vary in Luminance (L).
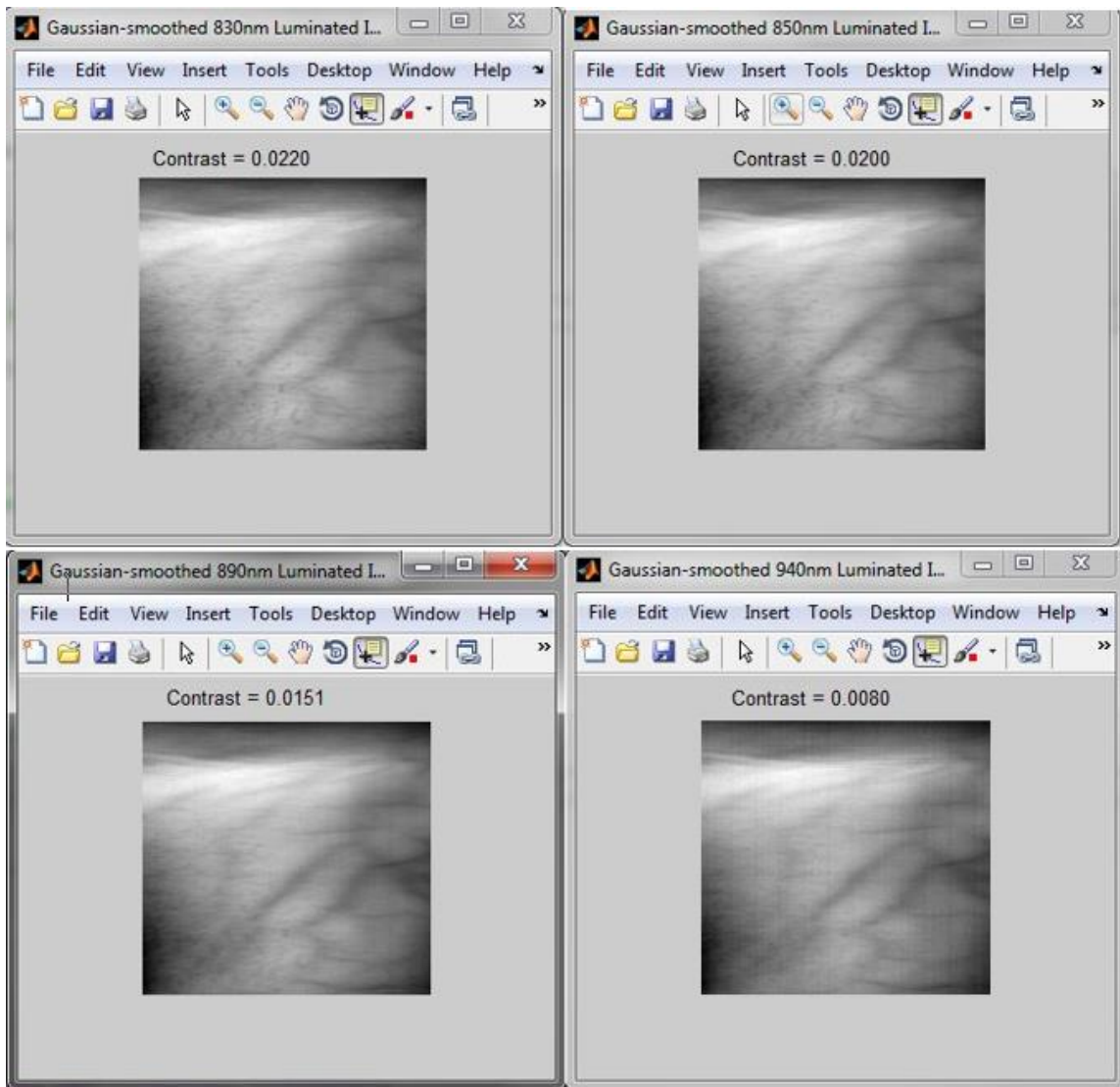
Figure 17: Multispectral images of a dark skin toned subject enhanced with (a) 830nm (b) 850nm (c) 890nm (d) 940nm

Figure 11 shows an enhancement in intensity contrast quality from the original image shown in Figure 10(a). It is observed that minute and discrete noise scatters in the image is eliminated or even meaned by the Gaussian normal distribution.

This justification applies to images of all skin tones, where even hidden or visibly topological parameters come to high visibility.
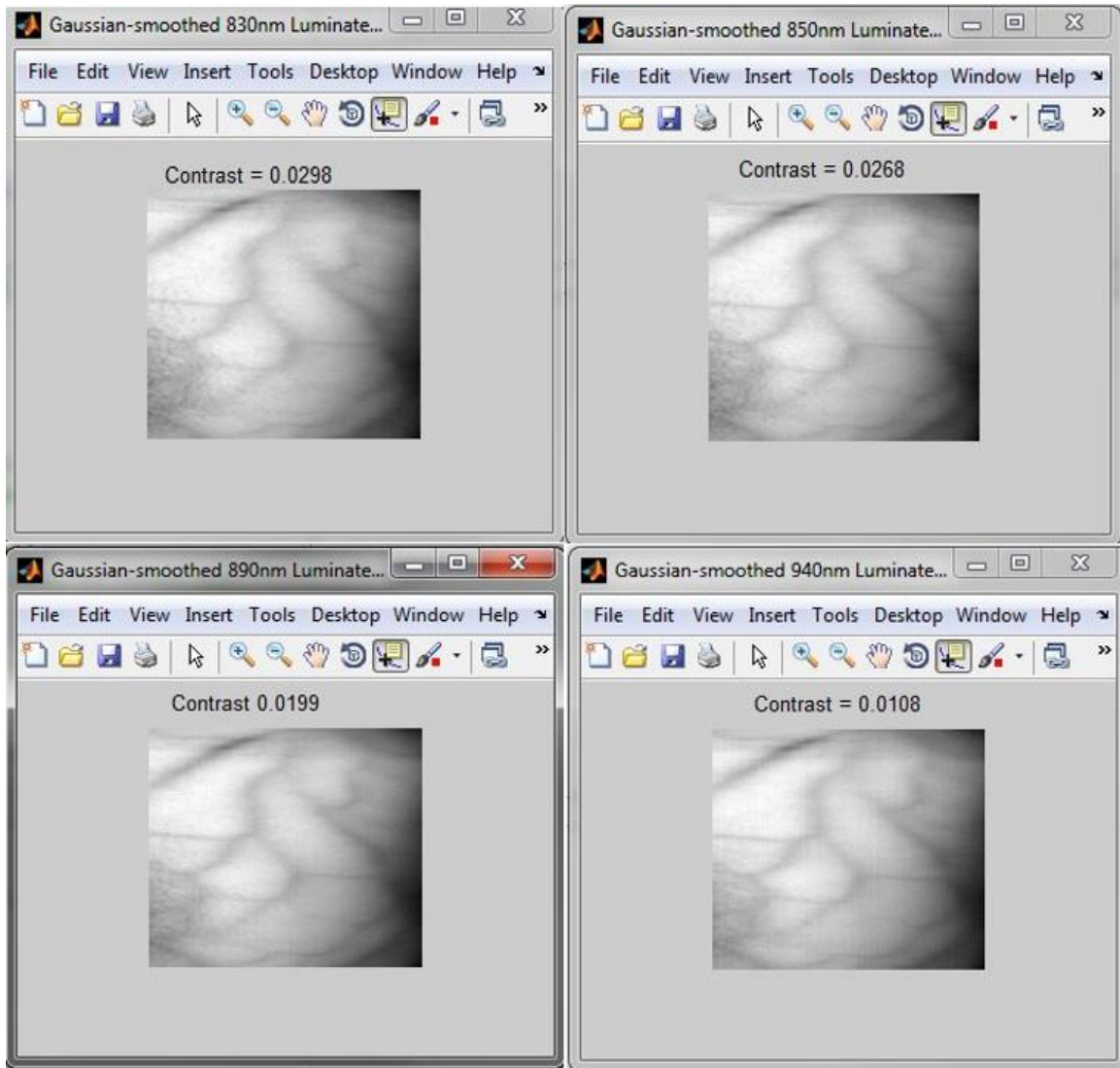
Figure 18: Multispectral images of a dark brown skin toned subject enhanced with (a) 830nm (b) 850nm (c) 890nm (d) 940nm
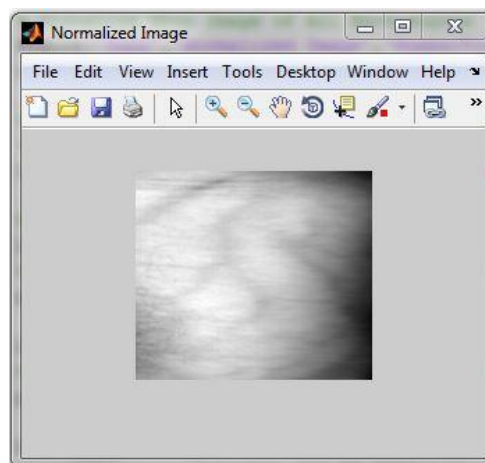
Figure 19: Original Multispectral (normalized) of a dark brown skin toned subject

Figure 12 displays enhancements in multiple folds of vein contrast from the original image of the subject as shown Figure 13.
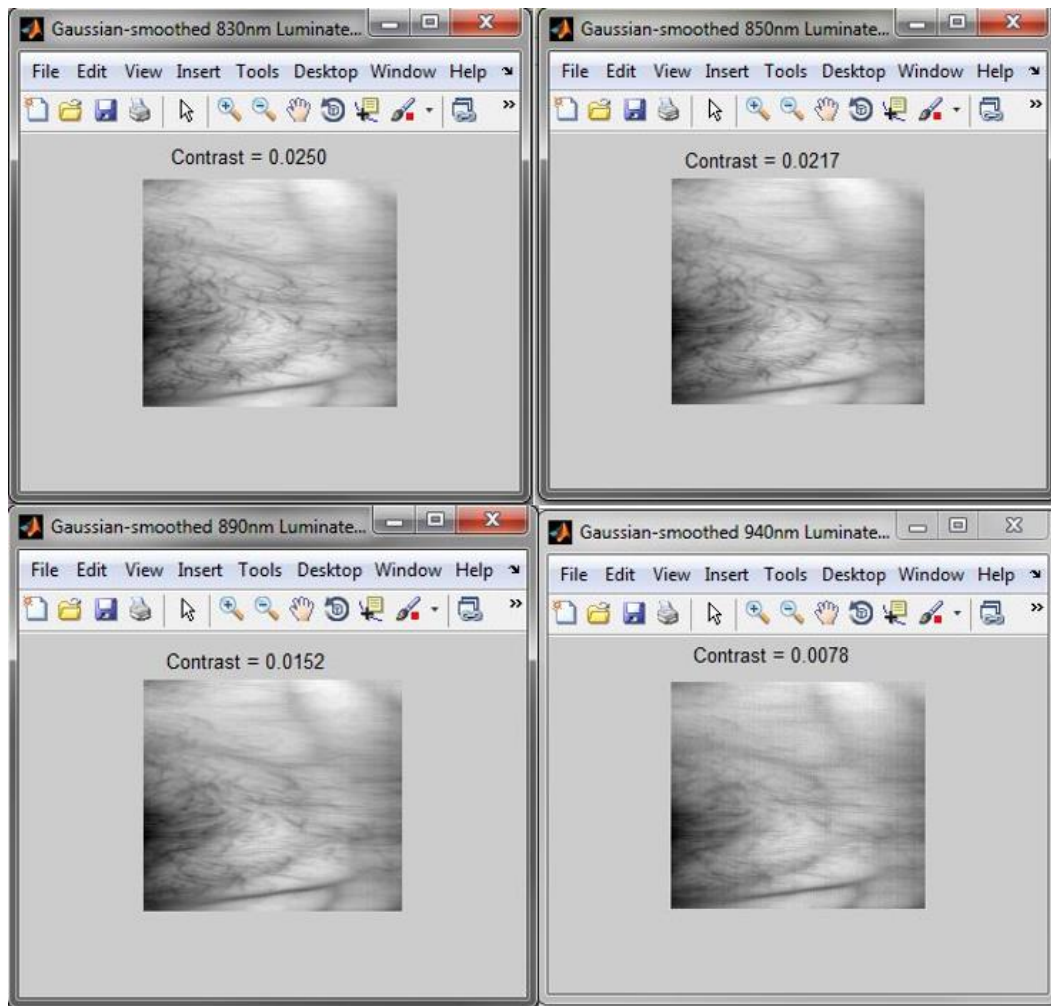
Figure 20: Multispectral images of a light brown skin toned subject enhanced with (a) 830nm (b) 850nm (c) 890nm (d) 940nm
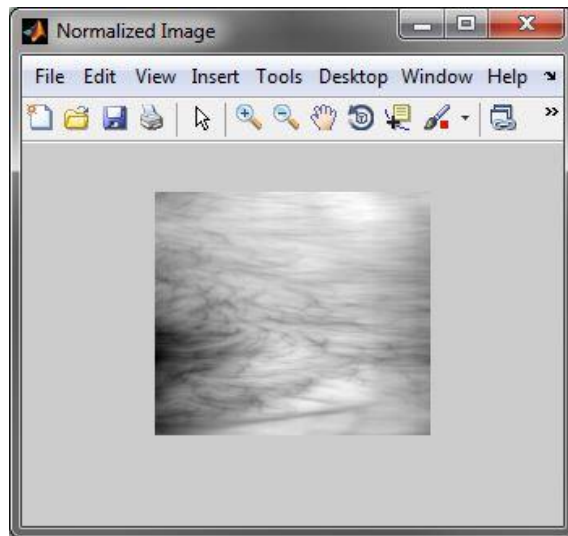
Figure 21: Original Multispectral (normalized) of a light brown skin toned subject
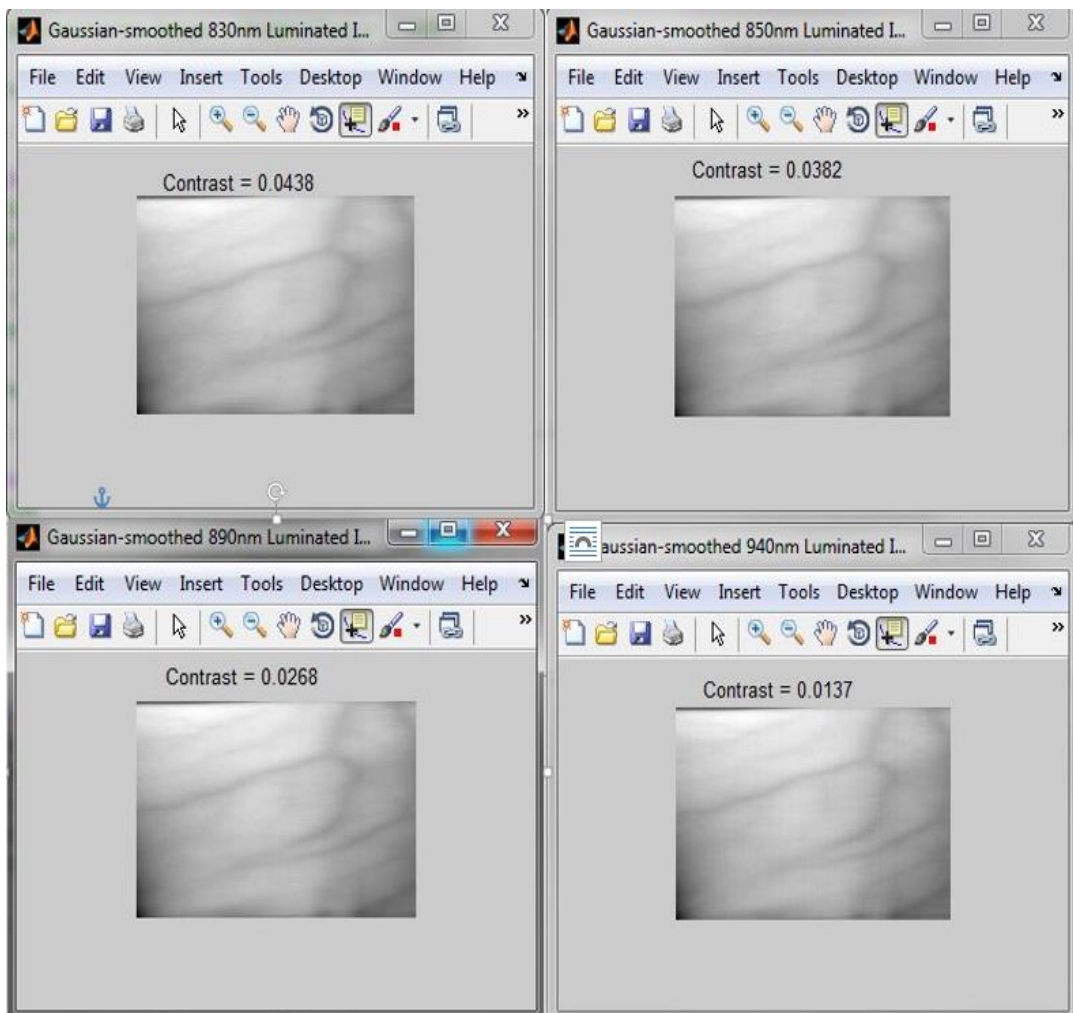
Figure 22: Multispectral images of a fair skin toned subject enhanced with (a) 830nm (b) 850nm (c) 890nm (d) 940nm
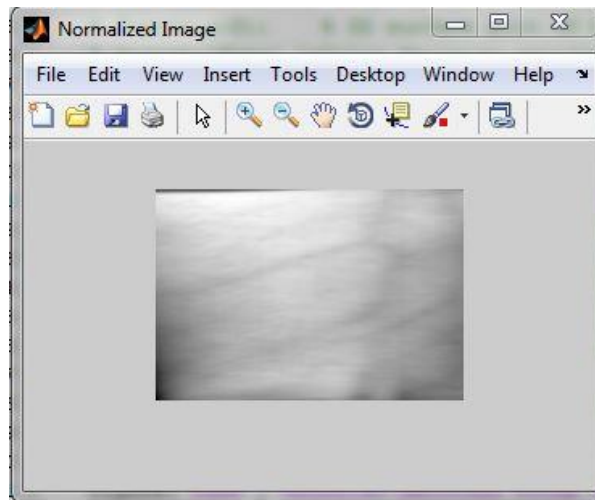
Figure 23: Original Multispectral (normalized) of a fair skin toned subject

4.3 Modelling Stage III – CLAHE Formulated Reflectance Algorithm Modelling

Contrast-Limited Adaptive Histogram Equalization (CLAHE) is a variant of the Adaptive Histogram Equalization (AHE), in which they are an evolution from the Histogram Equalization (HE) in the comparison that the adaptive method evaluate histograms from different segments (tiles) of an image. These histograms equalizes and redistribute the intensity values of the grayscale image, enhancing local contrasts [25]. Redistribution of pixel lightness intensity of the image extract discrete information on the ROI, where hidden topologies are more visible in a CLAHE-enhanced image.

However, the AHE method was prone to over-amplification of noises in the segments of an image with similar traits or medium. Hence, the Contrast-Limited Adaptive Histogram Equalization (CLAHE) overcomes this shortcoming by eliminating unnecessary amplifications by limiting the contrast enhancement. The Histogram smoothing characteristics in CLAHE contributes in eliminating spikes that result in large intensity fluctuation from one pixel to the next. Hence, this smoothing is a mean-effect to the neighbouring pixels of a homogenous segment region of an image ROI by using the Backward Variance Propagation technique.

The following is an example of a multispectral image enhanced with contrast-limited adaptive histogram equalization, where the information of interest (vessels) are more distinct and bold as compared to the original raw image, where noise is dominant.

28

(a)   (b)
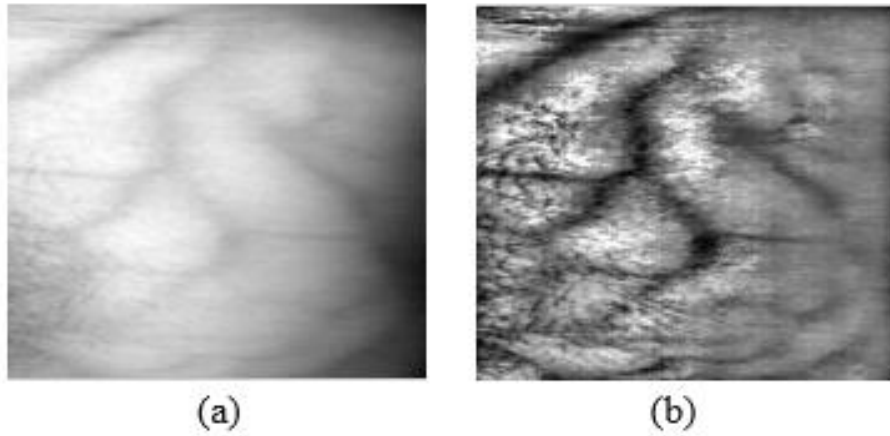
Figure 24: (a) Original Multispectral Image for Dark Brown Skinned Patient Meaned in the spectrum of 700nm-950nm (b) CLAHE Enhancement of the original image

(a)   (b)
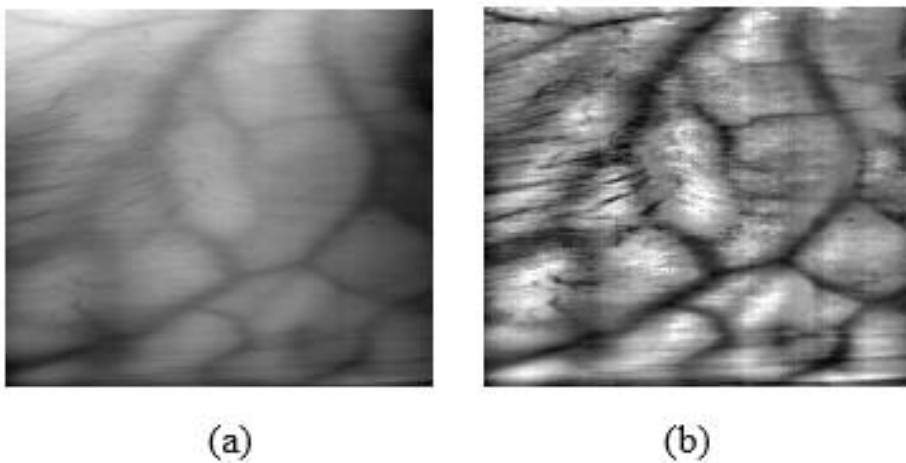
Figure 25: (a) Original Multispectral Image for Light Brown Skinned Patient Meaned in the spectrum of 700nm-950nm (b) CLAHE Enhancement of the original image
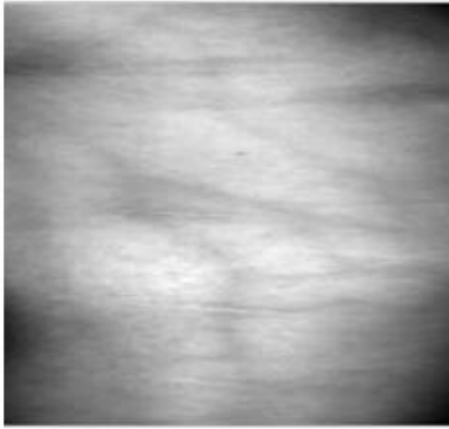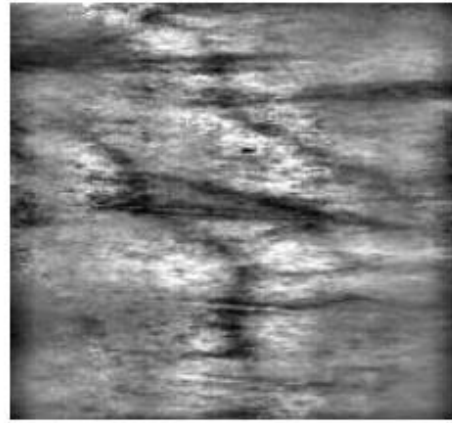
Figure 26: (a) Original Multispectral Image for Dark Skinned Patient Meaned in the spectrum ranging from 700nm to 950nm (b) CLAHE Enhancement of the original image
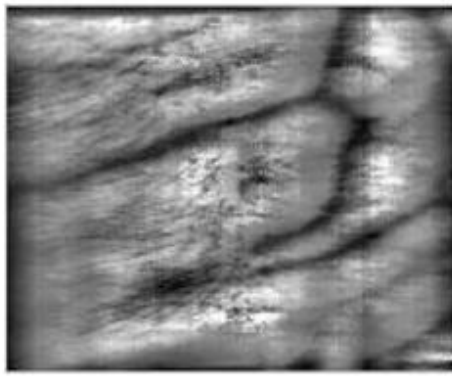
Figure 27: (a) Original Multispectral Image for Dark Skinned Patient Meaned in the spectrum ranging from 700nm to 950nm (b) CLAHE Enhancement of the original image
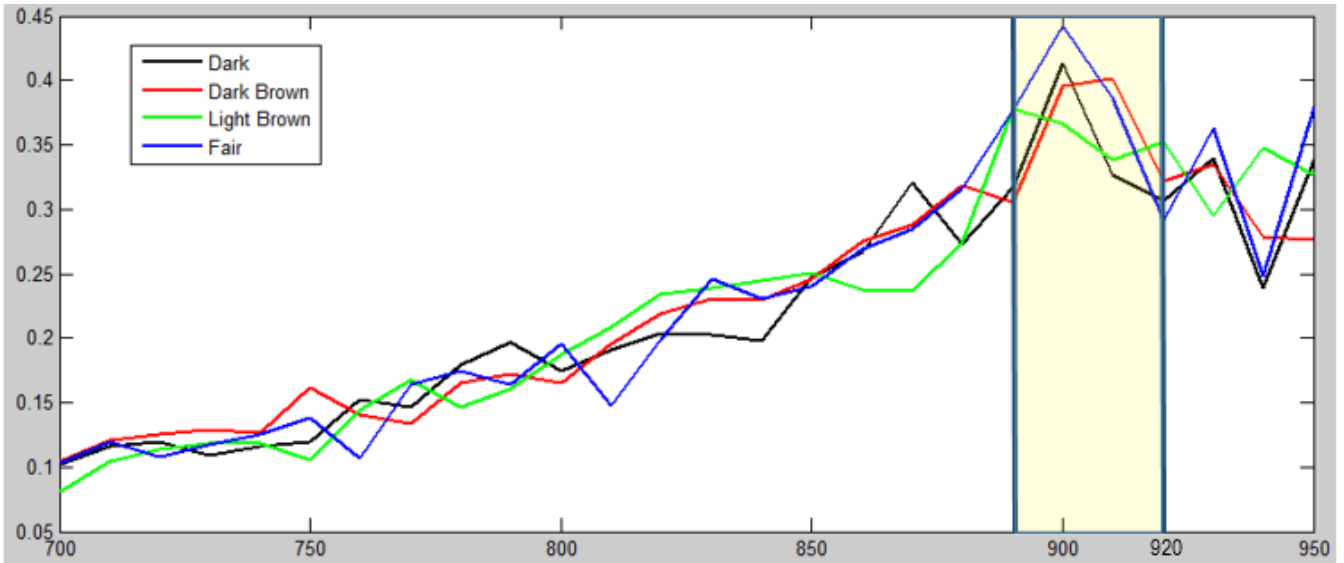
Figure 28: Trend for CLAHE Enhanced Reflectance Contrast of 8 Multispectral Images of each skin class; Fair, Light Brown, Dark Brown and Dark

Figure 28 possess almost the same trait as the trend in Figure 12, except that, overshoot spikes are very much reduced beyond the 920nm spectrum band, and the peak contrast at 890nm to 920nm is amplified after CLAHE enhancement. The histogram distribution across different homogenous segments of the image is unified by Backward Propagation of Variance (BPV) Histogram redistribution across the image pixels, eliminating strong noise spikes.

(a)   (b)
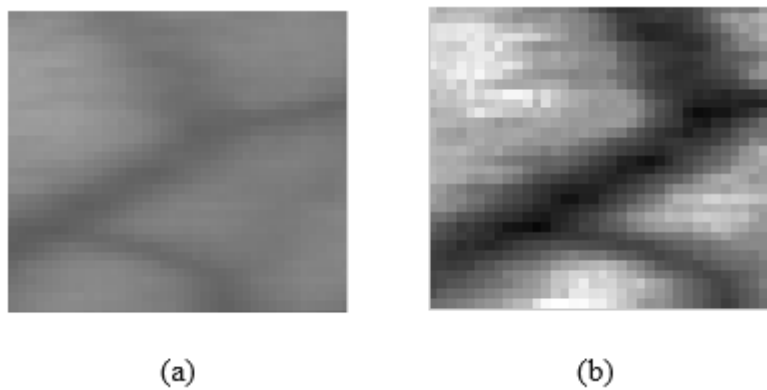
Figure 29: Histogram Equalization of intensity across pixel tiles (a) Original ROI (b) CLAHE Enhanced ROI

Figure 28 indicates the function of CLAHE in eliminating over amplification of noise by limiting contrast, and enhancing the image into a more distinct profiles of both vessel and skin tissue information. CLAHE is a suitable substitute to ridge detection algorithms and wide line detection algorithms, where it performs combination of both enhancement techniques.

To initialize the CLAHE algorithm, the `adapthisteq` function is used with specifications of `ClipLimit` where this parameter is normalized from [0 1] and the value selected for this modelling was 0.99 since higher index registered higher contrasts.

CLAHE enhancement scheme operates ROI by ROI in a loaded image, in the form of *tiles* rather than evaluating the whole image. Each *tile* or ROI contrasts is enhanced, so that the histogram of the selected region tallies with the histogram specification set by the 'Distribution' parameter. The neighbouring tiles are then combined using bilinear interpolation to remove artificially induced boundaries. Hence, the contrast in homogenous region can be limited to avoid strong spikes of noises that are scattered within the image pixels.
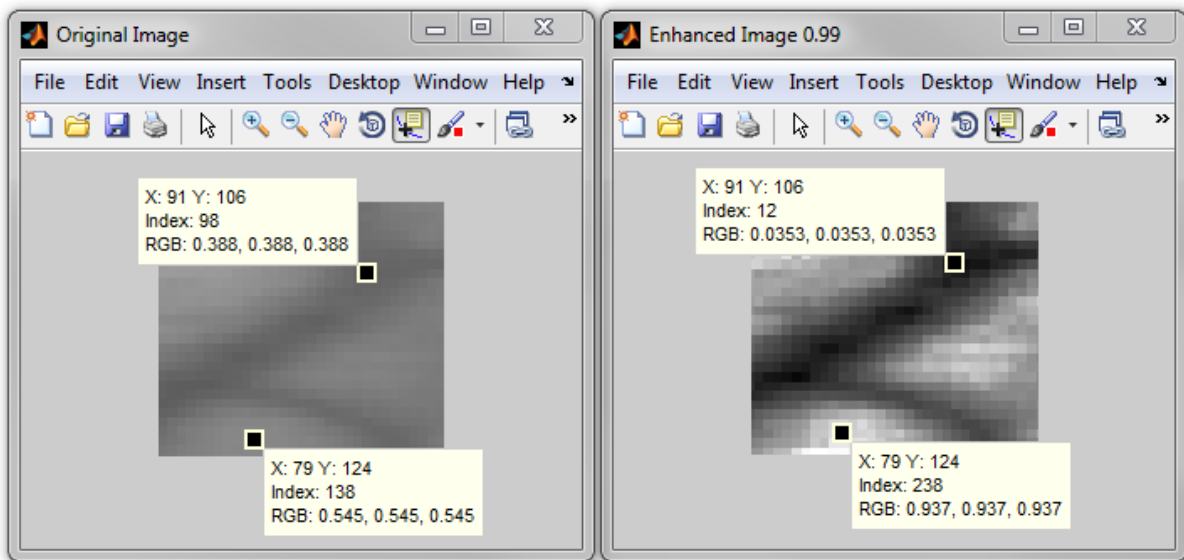
Figure 30: Comparison vessel-skin pixel intensity contrast between an original image and the CLAHE enhanced image.

4.4 Real Time Implementation
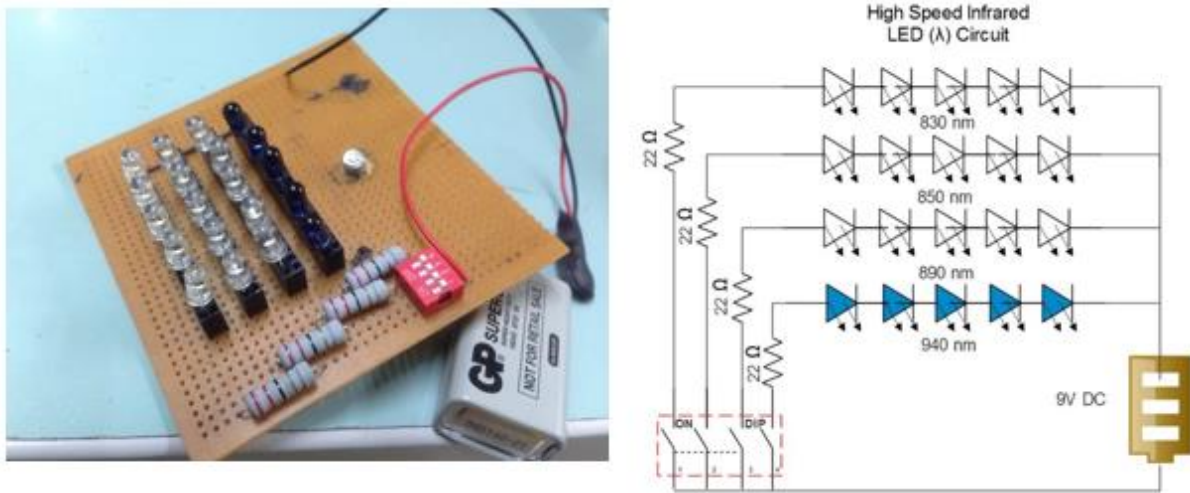
Figure 31: Dummy circuit construction to be tested during experimental testing of vein imaging based on Stage I Empirical Modelling.

The proven concept through series of modelling using reflectance, will then be introduced to the experimental testing of multispectral vein imaging in a real time approach.

The best selection (desired) illuminant, λ parameters will be translated into an illuminant circuit, which will be introduced into the experimental testing. This circuit will act as a dummy circuit till the LED's are installed into the Smart Vein Locator prototype, which is available in the Centre of Intelligent Signal & Imaging Research Cluster of University of Technology PETRONAS, Malaysia.
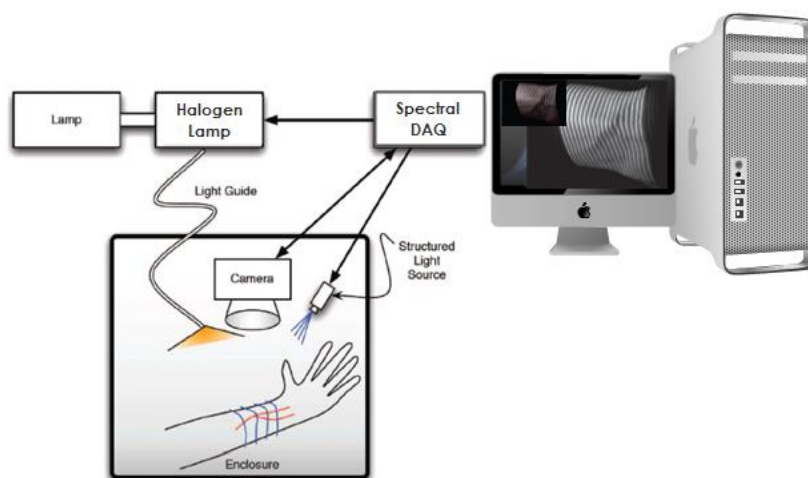
Figure 32: Experimental testing of illuminants during real-time spectral imaging.

Figure 33: Smart Vein Locator

4.5   Hypothesis

The hypothesis of this research is that, by using multiple illuminant sources, extraction of vein information is more efficient compared to the technique in previous literatures which used only one illuminant (wavelength) source. The usage of multiple illuminants or wavelengths in the NIR window allows spectral analysis in multiple resolutions, where vibrational light penetrates in many horizons of the hypodermal layer, detecting scarce properties veins in the forearm. An in-depth pixel extraction algorithms incorporated in all four stages of modelling has been an efficient method of obtaining an accurate index which helps in discriminating the vein and skin ROI uniquely.

CLAHE fine-tunes vessel identification by deploying its tile refragmentation and lightness redistribution equalizes reflectivity index of an image, eliminating unnecessary noise spikes, which could give about a false contrast trend. Hence, CLAHE enhancement scheme and incorporation of additional sets of optimum illuminants, as deduced in Stage I and III modelling catalyses automatic vessel extraction using Frangi Vesselness Filter.

4.6 Future Works

- Constrict to the study into a narrower spectroscopy, where the future approaches will unify illuminant source, using only single high speed IR LED.
- Work on incorporating selected illuminants into the Smart Vein Locator prototype for real time experimentation.
- Reanalyse the trend between 890nm-920nm for further effective classification of illuminants with respect to skin tones.
- Implement Frangi filter for vessel information extraction on CLAHE enhanced images.

5.0 REFERENCES

[1]   J. Song, C. Kim, and Y. Yoo, "Vein Visualization using a Smart Phone with Multispectral Wiener Estimation for Point-of-Care Applications," *Biomedical and Health Informatics, IEEE Journal of,* vol. PP, pp. 1-1, 2014.

[2]   G. Strangman, D. A. Boas, and J. P. Sutton, "Non-invasive neuroimaging using near-infrared light," *Biol Psychiatry,* vol. 52, pp. 679-93, Oct 1 2002.

[3]   A. J. Barton, G. Danek, P. Johns, and M. Coons, "Improving patient outcomes through CQI: vascular access planning," *J Nurs Care Qual,* vol. 13, pp. 77-85, Dec 1998.

[4]   L. Hadaway, "Infiltration and extravasation," *Am J Nurs,* vol. 107, pp. 64-72, Aug 2007.

[5]   F. P. Wieringa, F. Mastik, F. J. Cate, H. A. Neumann, and A. F. van der Steen, "Remote non-invasive stereoscopic imaging of blood vessels: first in-vivo results of a new multispectral contrast enhancement technology," *Ann Biomed Eng,* vol. 34, pp. 1870-8, Dec 2006.

[6]   F. Meriaudeau, V. Paquit, N. Walter, J. Price, and K. Tobin, "3D and multispectral imaging for subcutaneous veins detection," in *Image Processing (ICIP), 2009 16th IEEE International Conference on*, 2009, pp. 2857-2860.

[7]   V. C. Paquit, F. Meriaudeau, J. R. Price, and K. W. Tobin, "Simulation of skin reflectance images using 3D tissue modeling and multispectral Monte Carlo light propagation," in *Engineering in Medicine and Biology Society, 2008. EMBS 2008. 30th Annual International Conference of the IEEE*, 2008, pp. 447-450.

[8]   J. Jerome (Jerry) Workman, "An Introduction to Near Infrared Spectroscopy," Jul 1, 2014 2014.

[9]   Y. Ozaki, "Near-infrared spectroscopy--its versatility in analytical chemistry," *Anal Sci,* vol. 28, pp. 545-63, 2012.

[10]   R. R. Anderson and J. A. Parrish, "The Optics of Human Skin," *J Investig Dermatol,* vol. 77, pp. 13-19, 07//print 1981.

[11]   A. Shahzad, N. M. Saad, N. Walter, A. S. Malik, and F. Meriaudeau, "An efficient method for subcutaneous veins localization using Near Infrared imaging," in *Intelligent and Advanced Systems (ICIAS), 2014 5th International Conference on*, 2014, pp. 1-4.

[12]   Y. Taka, Y. Kato, and K. Shimizu, "Transillumination imaging of physiological functions by NIR light," in *Engineering in Medicine and Biology Society, 2000. Proceedings of the 22nd Annual International Conference of the IEEE*, 2000, pp. 771-774 vol.1.

[13]   A. B. Karpiouk, S. R. Aglyamov, S. Mallidi, W. G. Scott, J. M. Rubin, and S. Y. Emelianov, "Combined ultrasonic and photoacoustic imaging to age deep vein thrombosis: preliminary studies," in *Ultrasonics Symposium, 2005 IEEE*, 2005, pp. 399-402.

[14]   P. Beard, "Biomedical photoacoustic imaging," *Interface Focus,* vol. 1, pp. 602-31, Aug 6 2011.

[15]   A. Shahzad, N. Walter, A. S. Malik, N. M. Saad, and F. Meriaudeau, "Multispectral venous images analysis for optimum illumination selection," in *Image Processing (ICIP), 2013 20th IEEE International Conference on*, 2013, pp. 2383-2387.

[16]   M. Cope, P. van der Zee, S. R. Arridge, M. Essenpreis, C. E. Elwell, and D. T. Delpy, "Non-invasive measurement of tissue oxygenation using near infrared (NIR) spectroscopy," in *Optical Techniques and Biomedical Applications, IEE Colloquium on*, 1991, pp. 14/1-14/4.

[17]   I. Nishidate, A. Wiswadarma, Y. Hase, N. Tanaka, T. Maeda, K. Niizeki*, et al.*, "Noninvasive spectral imaging of skin chromophores based on multiple regression analysis aided by Monte Carlo simulation," *Opt Lett,* vol. 36, pp. 3239-41, Aug 15 2011.

[18]   H. D. Zeman, G. Lovhoiden, and C. Vrancken, "The clinical evaluation of vein contrast enhancement," *Conf Proc IEEE Eng Med Biol Soc,* vol. 2, pp. 1203-6, 2004.

[19]   H. D. Zeman, G. Lovhoiden, C. Vrancken, and R. K. Danish, "Prototype vein contrast enhancer," *Optical Engineering,* vol. 44, pp. 086401-086401-9, 2005.

[20]   V. C. Paquit, K. W. Tobin, J. R. Price, and F. Meriaudeau, "3D and multispectral imaging for subcutaneous veins detection," *Opt Express,* vol. 17, pp. 11360-5, Jul 6 2009.

[21]   F. Wang, A. Behrooz, M. Morris, and A. Adibi, "High-contrast subcutaneous vein detection and localization using multispectral imaging," *J Biomed Opt,* vol. 18, p. 50504, May 2013.

[22]   F. P. Wieringa, F. Mastik, and A. F. W. v. Steen, "Contactless Multiple Wavelength Photoplethysmographic Imaging: A First Step Toward "SpO2 Camera" Technology," *Annals of Biomedical Engineering,* vol. 33, pp. 1034-1041, 2005/08/01 2005.

[23]   I. Nishidate, T. Maeda, Y. Aizu, and K. Niizeki, "Visualizing depth and thickness of a local blood region in skin tissue using diffuse reflectance images," *J Biomed Opt,* vol. 12, p. 054006, Sep-Oct 2007.

[24]   Y. L. Katsogridakis, R. Seshadri, C. Sullivan, and M. L. Waltzman, "Veinlite transillumination in the pediatric emergency department: a therapeutic interventional trial," *Pediatr Emerg Care,* vol. 24, pp. 83-8, Feb 2008.

[25]   Muniyappan, S., et al. (2013). A novel approach for image enhancement by using contrast limited adaptive histogram equalization method. Computing, Communications and Networking Technologies (ICCCNT),2013 Fourth International Conference on.

[26]   Fadzil, M. A., et al. (2009). Thickness Characterization of 3D Skin Surface Images Using Reference Line Construction Approach. Visual Informatics: Bridging Research and Practice, Springer Berlin Heidelberg**:** 448-454.